Shear Flow Generation due to Electromagnetic Instabilities

M.Wakatani[1)], M.Sato[1)], N.Miyato[2)] and S.Hamaguchi[1)]
[1)]Graduate School of Energy Science, Kyoto University, Gokasho, Uji, 611-0011, Japan
[2)]Japan Atomic Energy Research Institute, Naka, Ibaraki, 311-0193, Japan
E-mail: wakatani@energy.kyoto-u.ac.jp

Abstract. Shear flow is the most important ingredient governing nonlinear behavior of many types of plasma instability. Electromagnetic effects on shear flow generation have been studied for an electromagnetic drift wave called resistive drift-Alfvén mode (RDAM) and a global MHD mode called resistive wall mode (RWM). For RDAM it is found that the generated shear flow stabilizes the dominant modes; however, other modes are destabilized. For RWM Maxwell stress due to magnetic fluctuations has a tendency to suppress the poloidal flow near the plasma surface, which gives almost same saturation level, since the shear flow stabilization disappears.

1.Introduction

Recent topics of plasma instabilities and induced anomalous transport in tokamaks and stellarators are related to the shear flow generation governing nonlinear saturation of fluctuations[1]. For nonlinear electrostatic drift waves such as resistive drift waves and ion temperature gradient driven drift modes, the most interesting result is the formation of zonal flow to suppress turbulent transport [2,3]. Here our concern is in the shear flow generation and nonlinear saturation of electromagnetic instabilities such as resistive drift-Alfvén modes (RDAMs) [4,5] and resistive wall modes (RWMs)[6,7,8]. The former is an electromagnetic drift wave which is considered as a candidate for the edge turbulence in tokamaks[9]. The latter is considered to limit the beta value in a steady operation of high bootstrap current tokamak with a negative shear[10]. Nonlinear fluid models are solved numerically for cylindrical plasmas, and characteristic behavior of both RDAMs and RWMs is discussed in the following.

2.Nonlinear RDAMs

For studying RDAMs we use the three field equations derived from Braginskii equations[11], which are composed of vorticity equation

$$\frac{n_0}{\omega_{ci}B_0}\left(\frac{\partial}{\partial t}+\mathbf{v}_E\cdot\nabla\right)\Omega-\frac{1}{e}\nabla_\parallel j_\parallel=0, \tag{1}$$

Ohm's law

$$\frac{\partial A}{\partial t}+\nabla_\parallel\phi-\frac{T_e}{ne}\nabla_\parallel n+\eta j_\parallel=0 \tag{2}$$

and continuity equation

$$\frac{\partial n}{\partial t}+\mathbf{v}_E\cdot\nabla n-\frac{1}{e}\nabla_\parallel j_\parallel=0, \tag{3}$$

where $j_\parallel=-(1/\mu_0)\nabla_\perp^2 A$, $\mathbf{v}_E=\hat{z}\times\nabla\phi/B_0$, $\Omega=\nabla_\perp^2\phi$, $\nabla_\parallel=\partial/\partial z-(\hat{z}\times\nabla A)/B_0\cdot\nabla$, $\omega_{ci}=eB_0/m_i$ is an ion cyclotron frequency, η is a resistivity. Here cold ions are assumed and toroidal magnetic curvature is neglected. For simplicity, single helicity is

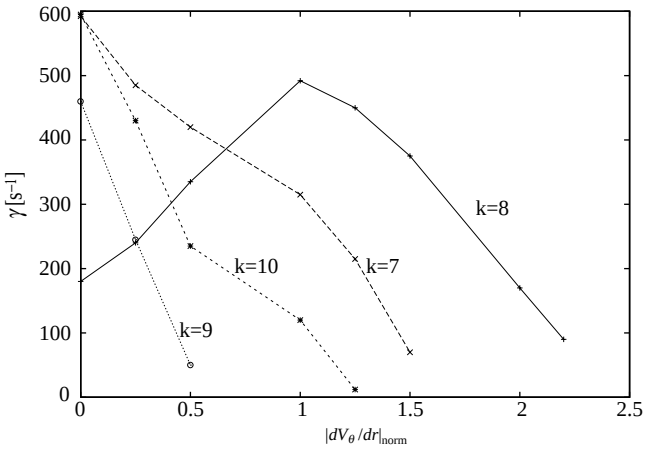

Figure 1. Linear growth rates of $k = 7$, 8, and 10 modes as a function of velocity shear. The flow profile is fixed at the time of saturation. The magnitude is changed to control $|dV_\theta/dr|_{\rm norm}$.

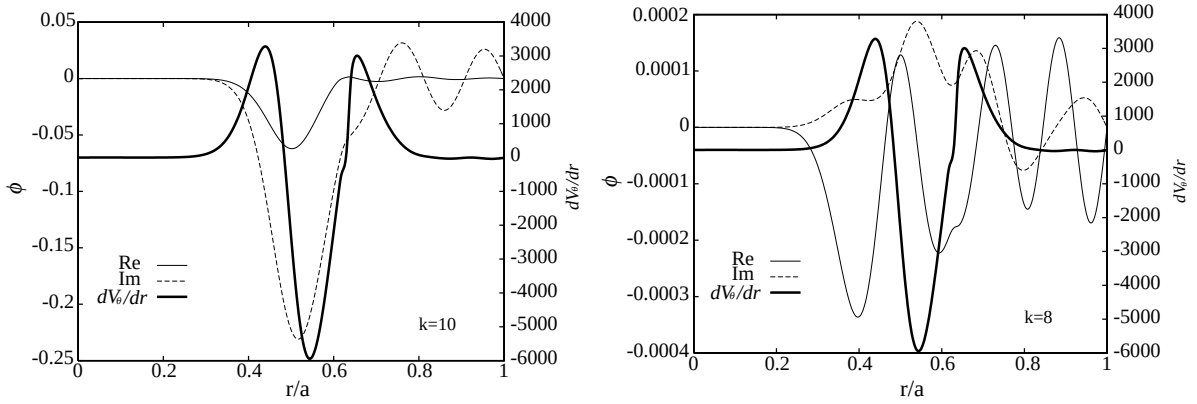

Figure 2. Radial profiles of electrostatic potential fluctuations for $k = 10$ and $k = 8$ modes, and poloidal flow shear at the saturation.

assumed in solving Eqs.(1)-(3). In the numerical calculations, mode numbers $(m, n) = (2k, k)$ are picked up for studying the RWMs destabilized near the $q = 2$ surface, where $0 \leq k \leq 10$ is assumed. Here $m(n)$ is a poloidal(toroidal) mode number. The fixed boundary conditions are assumed. Also a cylindrical tokamak is assumed with B_0 =1.0T, R =1.0m, a=0.2m, T_e=200eV, $n_0(r) = 5 \times 10^{20} \exp[-4.0(r/a)^2]$, $q(0)$=1.1 and $q(a)$ =4.2. In the numerical code, dissipative terms describing diffusion, resistivity and viscosity are included for obtaining nonlinear saturation of RDAMs. It is noted that the volume average beta is 0.018. Figure 1 shows the linear growth rates of k =7, 8 and 10 as a function of the maximum poloidal flow shear normalized by the saturated value. Here we have used the radial flow shear profiles shown in Fig.2, which are fixed for calculating the linear growth rates in Fig.1. The linear growth rates of the $k = 7$ and $k = 10$ modes decrease monotonically with the increase of the flow shear, and both modes are completely stabilized for $|V'_\theta|_{\rm norm} \gtrsim 2$. On the other hand, the growth rate of the $k = 8$ mode increases with the increase of the flow shear, although the $k = 8$ mode will be completely stabilized at $|V'_\theta|_{\rm norm} \simeq 2.5$. In Fig.2, the sheared poloidal flow at the saturation ($|V'_\theta|_{\rm norm}$=1 in Fig.1) seems sufficient to reduce both the linear growth rate of the most unstable $k = 10$ mode, and that of the secondary unstable $k = 7$ mode to about 1/5 and 1/2, respectively. However, the growth rate of $k = 8$ mode becomes more than twice by the sheared poloidal

flow ($|V'_\theta|_{\rm norm} = 1$ in Fig.1), and this mode keeps growing after the saturation. The difference between the poloidal shear flow effects on the RDAMs, stabilization on the $k = 7$ and 10 modes and destabilization on the $k = 8$ mode, is related to the radial mode structure of RDAM. Radial profiles of electrostatic potential $\tilde{\phi}$ for the $k = 10$ and $k = 8$ modes and the poloidal flow shear V'_θ are shown in Fig.2. The profile of $k = 10$ mode has the largest peak at $r/a \simeq 0.5$ which is near the largest peak of the poloidal flow shear. On the other hand, the largest peak of $k = 8$ mode is located at $r/a \simeq 0.4$ different from the largest peak of the flow shear. It is also noted that the width of radial mode structure seems wider than that of the flow shear profile for the $k = 8$ mode. These facts may explain the destabilizing effect of flow shear on RDAM.

3.Nonlinear RWMs

The reduced MHD equations for low beta cylindrical plasmas are obtained by neglecting the third term in Eq.(2). For studying nonliner RWMs equations for ϕ, A and η are solved. Resistivity is also introduced in the vacuum region to use the pseudo-vacuum model[12,13]. Time evolution of the resistivity in Eq.(2) is solved here. The equation for resistivity is assumed as

$$\frac{\partial \eta}{\partial t} = \mathbf{v} \cdot \nabla \eta + \kappa_\parallel \nabla_\parallel^2 \eta + \kappa_\perp \nabla_\perp^2 \eta + Q, \tag{4}$$

where the parallel diffusivity of resistivity $\kappa_\parallel$ is normalized with R^2/τ_{hp} and the perpendicular one $\kappa_\perp$ with a^2/τ_{hp}. For numerical calculations $\kappa_\parallel = 1$ and $\kappa_\perp = 10^{-5}$ are assumed. The source term Q is chosen as $\kappa_\perp \nabla_\perp^2 \eta_{eq}(r) + Q = 0$, where $\eta_{eq}(r)$ is a resistivity at an equilibrium state. It is possible to include a poloidal rotation in Eqs.(1),(2) and (4) with $\phi(r,t)$, since $V_\theta = -\partial\phi/\partial r$.

The pseudo-vacuum region is surrounded by the resistive wall with a finite thickness. In the resistive wall, the velocity is zero and the resistivity is independent of time. However, the poloidal flux may change in this region. It is also assumed that the outside of resistive wall is covered by a perfect conductor at r_c=2 for simplicity. That is, the main plasma is located in the region $r \leq 1$, the pseudo-vacuum in the region $1 < r < r_w$, and the resistive wall in the region $r_w \leq r \leq r_c$, where r_w is the boundary between the pseudo-vacuum and the resistive wall.

The current profile at an equilibrium state is chosen as $J_{eq}(r) = (J_a - J_b)(1 - r^{3.5})^2 + J_b$ for $0 \leq r \leq 1$, and $J_{eq}(r) = J_b \ll J_a$ for $1 < r < r_c$. The resistivity profile is assumed to be proportional to $1/J_{eq}(r)$ for $r < r_w$. $\eta(r = 0)$ and the resistivity in the pseudo-vacuum region η_v are set to be $\eta(0) = 10^{-5}$ and $\eta_v = 10^{-3}$, respectively. Resistivity of the resistive wall η_w is assumed to be $\eta_w = 10^{-4}$. For numerical calculations, q_a=1.85 and r_w=1.2 are assumed, where q_a is a safety factor at the plasma surface. The rational surface of $q = 2$ is located at $r = r_s \simeq 1.04$ in the pseudo-vacuum region.

When a perfect conducting wall is located at $r \leq 1.27$ instead of a resistive wall, the ideal kink mode can be stabilized perfectly. When a resistive wall is assumed, RWMs become always unstable. However, RWM can be stabilized by a rigid poloidal rotation. Figure 5 shows the time evolution of magnetic energy of $(m, n) = (2, 1)$ mode for $r_w = 1.2$. For $\omega_{eq} \geq 1.2 \times 10^{-2}$ the nonlinear growth rate is enhanced when the magnetic fluctuation exceeds a critical level, and the saturated amplitude becomes comparable to that in the case of $\omega_{eq} \simeq 0$. It is noted that a rigid poloidal rotation with $\phi(r) \propto r^2$ is assumed initially.

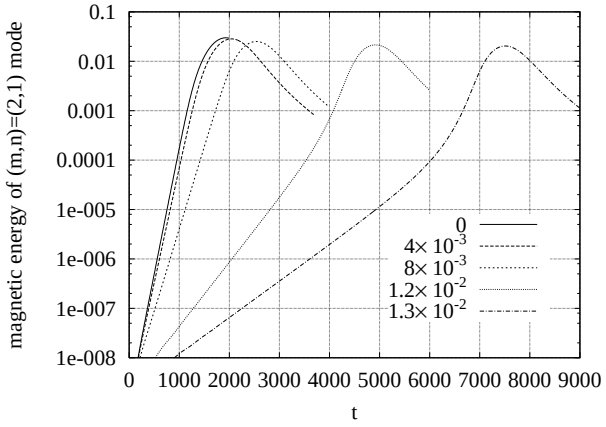

Figure 3. Time evolution of magnetic energy of $(m, n) = (2, 1)$ mode for $r_w = 1.2$ for various poloidal rotation frequency.

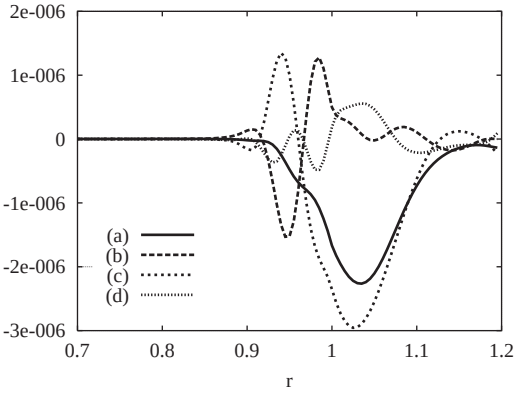

Figure 4. Radial profiles of each term in Eq.(10) at t=6000 for $\omega_{eq} = 1.3\times10^{-2}$. (a) $\partial\langle V_\theta\rangle/\partial t$, (b) $-(1/r^2)\partial/\partial r r^2\langle\tilde{V}_r\tilde{V}_\theta\rangle$, (c) $(1/r^2)\partial/\partial r r^2\langle\tilde{B}_r\tilde{B}_\theta\rangle$ and (d) $-\nu d\tilde{U}_0/dr$.

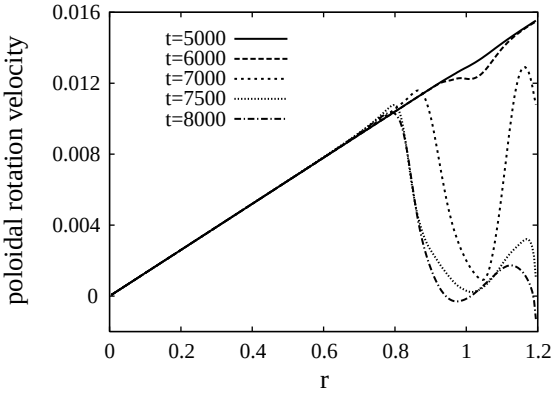

Figure 5. Time evolution of profile of poloidal velocity for $r_w = 1.2$ and $\omega_{eq} = 1.3 \times 10^{-2}$.

From Eq.(1), the time evolution of average poloidal velocity $\langle V_\theta\rangle$ is given by

$$\begin{aligned}\frac{\partial\langle V_\theta\rangle}{\partial t} = &-\frac{1}{r^2}\frac{\partial}{\partial r}r^2\langle\tilde{V}_r\tilde{V}_\theta\rangle \\ &+\frac{1}{r^2}\frac{\partial}{\partial r}r^2\langle\tilde{B}_r\tilde{B}_\theta\rangle - \nu\frac{d\tilde{U}_0}{dr},\end{aligned} \tag{5}$$

where $\langle f\rangle = \int_0^{2\pi}\int_0^{2\pi} f d\theta dz/4\pi^2$ and $\tilde{U}_0$ is $(m, n) = (0, 0)$ component of perturbed vorticity. Here the viscous term is added with a viscosity ν. Figure 3 shows each terms in Eq.(5) at t=6000 for $\omega_{eq} = V_\theta/r = 1.3 \times 10^{-2}$. The left hand side of Eq.(5) give a damping force in the vicinity of the rational surface (see Fig.4(a)) mainly due to the magnetic Reynolds stress or Maxwell stress (see Fig.4(c)). The electrostatic Reynolds stress (see Fig.4(b)) has a tendency to generate the poloidal flow. However its contribution is weak. Also the viscosity affects to generate the poloidal flow near the rational surface (see Fig.4(d)). Figure 5 shows the time evolution of the profile of poloidal rotation velocity. The slowdown of poloidal rotation can be clearly seen as shown in Fig.5, as the minimum of poloidal

rotation velocity decreases to almost zero. Then the stabilizing effect of the poloidal rotation becomes weak. This leads to the enhanced growth rate before the saturation. It is noted that the RWM is linearly stabilized for $\omega_{eq} \geq 1.4 \times 10^{-2}$.

4.Discussion

It is recognized that the poloidal shear flow or zonal flow is generated by the Reynolds stress due to the electrostatic drift waves. Here the electromagnetic effect on the shear flow generation has been studied for the resistive drift Alfvén modes. It is confirmed that the electromagnetic fluctuations produce Maxwell stress which has a tendency to suppress the poloidal shear flow. An interesting result is that the poloidal shear flow destabilizes the resistive drift Alfvén mode, when the radial mode structure is wider than the flow shear profile, and the peak of the flow shear is shifted from that of the radial mode structure.

The poloidal shear flow also has stabilizing effects on global MHD modes. Here it is shown that the resistive wall mode is stabilized linearly; however, the nonlinear saturation level of RWM does not depend on the poloidal rotation frequency. This result is explained by the Maxwell stress which has a role to suppress the poloidal shear flow. When the RWM grows, Maxwell stress is increased and the poloidal flow is decreased to almost zero in the neighborhood of plasma surface. Then the growth rate is enhanced nonlinearly.

It seems necessary to study electromagnetic effects on the generation or decay of shear flow for understanding behavior of finite beta plasmas in tokamaks and stellarators.

Acknowledgement
This work was supported by the Grant-in-Aid for Scientific Research (c) of the Ministry of Education, Culture, Sports, Science and Technology, Japan.

References

[1] P.W.Terry, Rev. Mod. Physics **72** (2000) 109.
[2] A.Hasegawa and M.Wakatani, Phys. Rev. Lett. **59** (1987) 1581.
[3] Z.Lin et al., Science **281** (1998) 1835.
[4] J.T.Tang and N.C.Luhmann,Jr., Phys. Fluids **19** (1976) 1935.
[5] N.Miyato, S.Hamaguchi and M.Wakatani, Plasma Phys. Control. Fusion (to be published).
[6] J.M.Finn, Phys. Plasmas **2** (1995) 198.
[7] R.Fitzpatrick and A.Y.Aydemir, Nucl. Fusion **36** (1996) 11.
[8] A.Yoshioka, T.Tatsuno and M.Wakatani, J. Phys. Soc. Jpn **67** (1998) 3794.
[9] O.Pogutse, Yu.Igitkhanov, G.Janeschitz and J.G.Cordey, Plasma Phys. Control. Fusion **21**A (1997) 1041.
[10] A.M.Garofaro et al., Phys. Plasmas **6** (1999) 1893.
[11] R.D.Hazeltine, Phys. Fluids **26** (1983) 3242.
[12] G. Kurita et al., Nucl. Fusion **26** (1986) 449.
[13] Yu. N. Dnestrovskii et al., Sov. J. Plasma Phys. **11** (1985) 616.